

# Paleoceanography and Paleoclimatology











## RESEARCH ARTICLE

10.1029/2023PA004720

## Northeastern Caribbean Rainfall Variability Linked to Solar and Volcanic Forcing

### Key Points:

- Speleothem-based Puerto Rican rainfall reconstruction shows prominent multidecadal-to-centennial variability during the past five centuries
- Puerto Rican rainfall fluctuations are linked to solar variations before the eighteenth century and volcanic forcing thereafter
- Caribbean Sea-surface temperature anomalies as part of the Atlantic Multidecadal Variability emerge as robust precursor of rainfall amounts

Rolf Vieten<sup>1</sup> , Sophie F. Warken<sup>2,3</sup> , Davide Zanchettin<sup>4</sup> , Amos Winter<sup>1,4,5</sup> , Denis Scholz<sup>6</sup> , David Black<sup>7</sup> , Gabriella Koltai<sup>8</sup> , and Christoph Spötl<sup>8</sup> 

<sup>1</sup>Department of Marine Sciences, University of Puerto Rico, Mayaguez, PR, USA, <sup>2</sup>Institute of Environmental Physics, Heidelberg University, Heidelberg, Germany, <sup>3</sup>Institute of Earth Sciences, Heidelberg University, Heidelberg, Germany, <sup>4</sup>Department of Environmental Sciences, Informatics and Statistics, University Ca'Foscari of Venice, Venice, Italy, <sup>5</sup>Department of Earth and Environmental Systems, Indiana State University, Terre Haute, IN, USA, <sup>6</sup>Institute for Geosciences, University of Mainz, Mainz, Germany, <sup>7</sup>School of Marine and Atmospheric Sciences, Stony Brook University, Stony Brook, NY, USA, <sup>8</sup>University of Innsbruck, Institute of Geology, Innsbruck, Austria

### Supporting Information:

Supporting Information may be found in the online version of this article.

### Correspondence to:

S. F. Warken,  
swarken@iup.uni-heidelberg.de

### Citation:

Vieten, R., Warken, S. F., Zanchettin, D., Winter, A., Scholz, D., Black, D., et al. (2024). Northeastern Caribbean rainfall variability linked to solar and volcanic forcing. *Paleoceanography and Paleoclimatology*, 39, e2023PA004720. <https://doi.org/10.1029/2023PA004720>

Received 13 JULY 2023

Accepted 23 MAR 2024

### Author Contributions:

**Conceptualization:** Rolf Vieten,

Davide Zanchettin, Amos Winter

**Formal analysis:** Davide Zanchettin, Amos Winter

**Funding acquisition:** Amos Winter, Denis Scholz, David Black

**Investigation:** Rolf Vieten, Sophie

F. Warken, Davide Zanchettin, Amos Winter, Denis Scholz, David Black, Gabriella Koltai

**Methodology:** Davide Zanchettin, Amos Winter

**Project administration:** Amos Winter

**Resources:** Sophie F. Warken, Amos Winter, Denis Scholz, David Black, Christoph Spötl

**Abstract** We present a 500-year precipitation-sensitive record based on co-varying speleothem  $\delta^{18}\text{O}$  values and Mg/Ca ratios from Larga cave in Puerto Rico. This multi-proxy record shows that the evolution of rainfall in the northeastern Caribbean was characterized by alternating centennial dry and wet phases corresponding to reduced versus enhanced convective activity. These phases occurred synchronous with relatively cool and warm tropical Atlantic sea-surface temperatures (SSTs), respectively. While the observed pattern suggests a close link of northeastern Caribbean rainfall to the Atlantic Multidecadal Variability, a regional comparison reveals intermittent regional heterogeneity especially on decadal timescales, which may be related to a superimposing influence of the Pacific and Atlantic basins. Furthermore, the speleothem-based hydroclimate reconstruction indicates a significant volcanic impact during the past two centuries, and further reveals a potential solar signal in the preceding three centuries. We posit that the forcing likely shifted from solar to volcanic during the eighteenth century in being an important source of multidecadal to centennial Caribbean rainfall variability. The link between convective rainfall and natural forcing may be explained through a modulation of SST variations in the tropical Atlantic and Pacific oceans.

**Plain Language Summary** Climate change is expected to affect rainfall throughout the Caribbean and Central America, where over 200 million people are heavily dependent upon rain as their main source of freshwater. We have looked at how the amount of rainfall in the Caribbean has changed through time, and possible reasons for these changes, to inform predictions of future rainfall patterns for the region. Cave mineral deposits, also known as speleothems, can be used to assess the amount of regional rainfall in the past by looking at their slight changes over time in the mineral's chemical composition. We created a record of Caribbean rainfall spanning the last five centuries using a speleothem from Puerto Rico. Our results indicate that rainfall changes since the sixteenth century were strongly influenced by changes in temperatures of the surface waters of the Atlantic Ocean. We further found that changes in the sun's brightness and volcanic eruptions may alter Atlantic Ocean sea-surface temperature, which in turn affect the overall changes in Caribbean rainfall patterns.

## 1. Introduction

Late Holocene hydroclimate reconstructions in Central America and the Caribbean have reported substantial decadal to centennial variations in precipitation amount, but the dominant drivers of these rainfall changes are still debated, and may be spatially and temporally heterogeneous (e.g., Asmerom et al., 2020; Bhattacharya & Coats, 2020; Obrist-Farner et al., 2023; Steinman et al., 2022; Yang et al., 2024). This uncertainty is partly due to the lack of well-dated, high resolution paleoclimate reconstructions prior to the twentieth century, in particular in the north-eastern Caribbean (Obrist-Farner et al., 2023; Oster et al., 2019; Steinman et al., 2022). The spatial and temporal distribution of rainfall in Central America and the Caribbean is mainly controlled by the Inter-Tropical Convergence Zone (ITCZ) and the North Atlantic Subtropical High (NASH), which are responsible for the characteristic seasonal cycle with enhanced convection, cyclogenesis, and associated rainfall amounts in the warm summer season (Martinez et al., 2019). In addition, their long-term variability affects rainfall patterns and tropical cyclone (TC) activity on decadal to centennial timescales (Hernández Ayala, 2019; Pausata & Camargo, 2019; Taylor et al., 2002; Yang et al., 2024).

© 2024 The Authors.

This is an open access article under the terms of the [Creative Commons Attribution-NonCommercial License](https://creativecommons.org/licenses/by/4.0/),

which permits use, distribution and reproduction in any medium, provided the original work is properly cited and is not used for commercial purposes.

**Software:** Davide Zanchettin  
**Supervision:** Amos Winter  
**Validation:** Sophie F. Warken  
**Visualization:** Sophie F. Warken,  
 Davide Zanchettin  
**Writing – original draft:**  
 Davide Zanchettin, Amos Winter  
**Writing – review & editing:** Sophie  
 F. Warken, Davide Zanchettin,  
 Amos Winter, Denis Scholz, David Black,  
 Gabriella Koltai, Christoph Spötl

In the northeastern Caribbean, Puerto Rican speleothem records covering different time slices over the past 46 ka suggest that multidecadal to centennial rainfall changes are closely associated with Atlantic sea surface temperature (SST) variations (Vieten et al., 2024; Warken et al., 2020, 2022b; Winter et al., 2011). Other regional high-resolution hydroclimate records located in the western Caribbean or Central America support the general interpretation that late Holocene multidecadal SST variations in the tropical Atlantic and Caribbean are an important precursor of convective rainfall changes in the region (Fensterer et al., 2012; Winter et al., 2015; Wright et al., 2022). Tropical Atlantic SST variations are part of the basin-scale phenomenon known as Atlantic Multidecadal Variability (AMV, also denoted as Atlantic Multidecadal Oscillation, AMO) (Kilbourne et al., 2008; Vásquez-Bedoya et al., 2012; Waite et al., 2020; Wang et al., 2006, 2017). As a consequence, multidecadal rainfall variations in the eastern Caribbean and the wider realm have been related to the AMV (e.g., Fensterer et al., 2012; Hernández Ayala, 2019; Stephenson et al., 2014; Taylor et al., 2002; Winter et al., 2011).

In addition, paleoclimate records and modeling studies suggest a significant influence of competing effects of Atlantic and Pacific SSTs and associated teleconnection patterns (e.g., Bhattacharya & Coats, 2020; Lachniet et al., 2017; Sullivan et al., 2021; van Beynen et al., 2007; Wright et al., 2022). As a result, coupled phenomena in the tropical and extra-tropical Pacific, most prominently including the El Niño Southern Oscillation (ENSO) as well as the Pacific Decadal Variability (PDV), may modulate Caribbean rainfall patterns on different timescales (Kim et al., 2020; van Beynen et al., 2007). A separation Atlantic and Pacific influences on Caribbean rainfall is, however, complicated due to variable interdependencies between modes of oceanic and SST variability in both basins (Hernández et al., 2020; Taylor et al., 2002; Zhang & Delworth, 2007). Further complexity arises because the cross-basin relationships of tropical Atlantic and Pacific SSTs as well as the observed PDV-AMV connection may not be a persistent feature of inter-basin variability, as suggested by numerical simulations (Meehl et al., 2021; Zanchettin, Bothe, Rubino, & Jungclaus, 2016). In addition, there is large inter-model uncertainty in the simulated AMV influence on the equatorial Pacific (e.g., Ruprich-Robert et al., 2021), and several mechanisms acting on different timescales have been proposed to explain a potential AMV-ENSO connection (e.g., Zanchettin, Bothe, Graf, et al., 2016). Attribution of AMV and PDV as predominantly externally forced rather than intrinsic modes of variability remains debated, although a host of observational, proxy- and model-based studies suggest the AMV to be more sensitive to natural and anthropogenic external forcing than the PDV (Fang et al., 2021; Mann et al., 2020; Otterå et al., 2010; Zhang et al., 2013).

In this respect, evidence of a dominant influence of natural forcing, that is, solar activity and energetic volcanic eruptions, on Caribbean multidecadal to centennial SSTs and hydroclimate changes has been found by a number of studies (Black et al., 1999; Burn & Palmer, 2014; Haase-Schramm et al., 2003; Hodell et al., 2001; Pollock et al., 2016; Ridley et al., 2015; Smirnov et al., 2017; Waite et al., 2020; Warken et al., 2021; Winter et al., 2015; Yang et al., 2024). For example, a reconstruction of Mesoamerican precipitation based on a speleothem record from the Yucatán Peninsula revealed a strong association between the occurrence of multidecadal drying phases during the past three centuries and clusters of strong tropical volcanic eruptions (Winter et al., 2015). Yet, over the modern era, the effects of solar and volcanic forcing are masked by increasing anthropogenic impact (Ridley et al., 2015; Schmidt et al., 2011). Hence, the dominating processes of tropical precipitation and the potential relation with SSTs, AMV/PDV, and forcing mechanisms prior to the nineteenth century are still uncertain. This is also because of the limited temporal and spatial coverage of available studies considering the known non-stationarity of teleconnections and dependency of responses on initial conditions and mean climate state (e.g., Swingedouw et al., 2015; Zanchettin et al., 2013).

Here we provide a high-resolution multiproxy-based reconstruction of precipitation amount from Larga cave, Puerto Rico, spanning the past five centuries, increasing the spatial and temporal coverage and resolution of north-eastern Caribbean precipitation reconstructions. This record enables us to (a) identify a predominant multidecadal to centennial component in regional precipitation, (b) discuss Caribbean precipitation in relation to Caribbean SSTs and the AMV, and (c) assess natural forcings on Mesoamerican/Caribbean precipitation back to about 1500 AD.

## 2. Materials and Methods

### 2.1. Sample Description

Larga cave is located at a height of 350 m above sea level in the north-central karst region of Puerto Rico (N 18°19'; W 66°48') (Figure 1a). The area is a mature karst characterized by sinkholes and mogotes. A thick tropical forest covers the surface above the cave, which is dominantly vadose with some phreatic features. The cave developed in

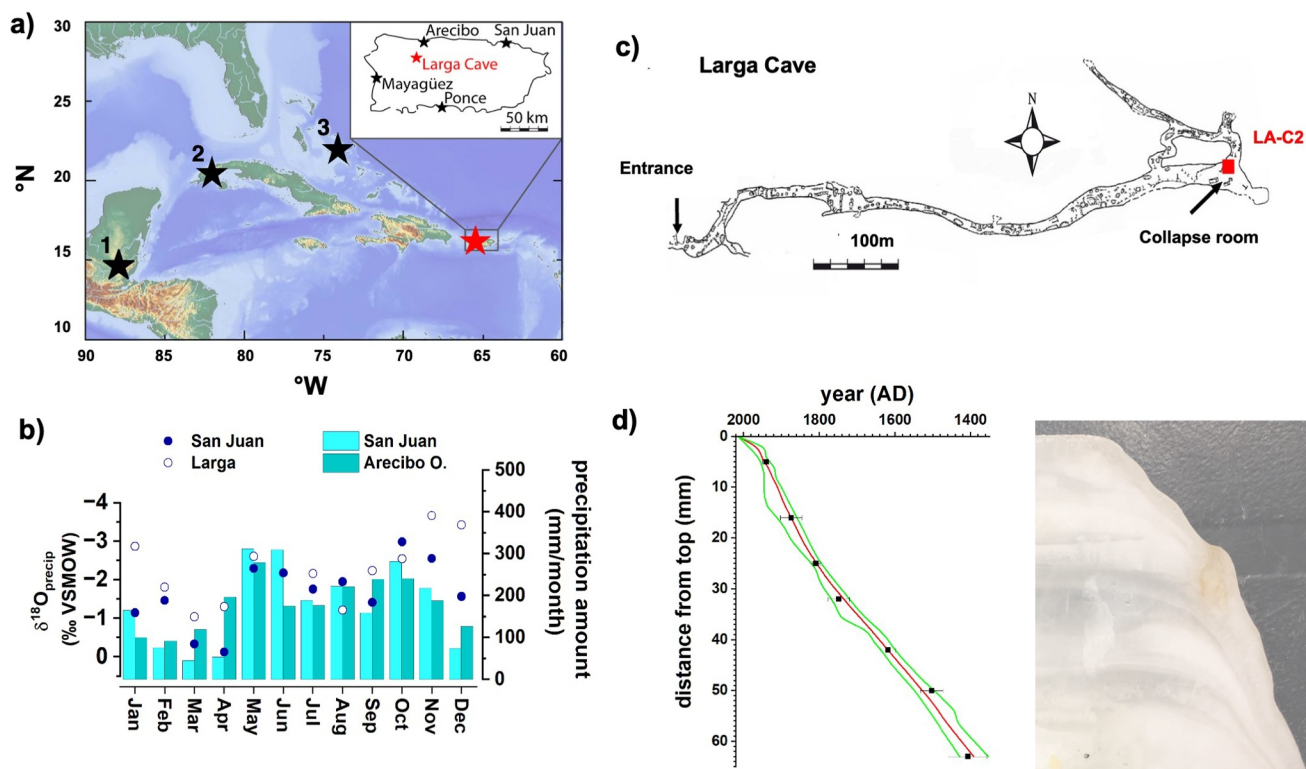


**Figure 1.** (a) Map showing the locations of Larga (red star) and of other relevant records discussed in this study: (1) Xibalba cave (Winter et al., 2015); (2) Santo Tomas Cave (Fensterer et al., 2012); (3) Lee Stacking Island, Bahamas (Waite et al., 2020). The inset displays the position of Larga cave and meteorological stations in Puerto Rico. (b) Monthly normals of precipitation amount at Arecibo and GNIP station San Juan compared to rainfall  $\delta^{18}\text{O}$  values at San Juan and Larga Cave (see text for details and references). (c) Plan view of Larga cave (after Miller, 2010) indicating the collection site; (d)  $^{230}\text{Th}/\text{U}$ -ages and age-depth-model obtained by StalAge (Scholz & Hoffmann, 2011) (red line, green lines are 95%-confidence limits). The age model is compared to a scan of the upper right half of a longitudinal section of speleothem PR-LA-C2.

the Oligocene Lares Limestone (Monroe, 1980). Speleothem PR-LA-C2 (Figure 1d) was collected in 2014 at site LA-C2 (Figure 1c). At this location, in the back of the cave, the seasonal, temperature-related cave air ventilation is minimal, and cave air temperature is stable ( $23.4 \pm 0.2^\circ\text{C}$ ; Vieten, Warken, Winter, Scholz, et al., 2018; Vieten et al., 2016). Over the cave monitoring period between 2013 and 2019, the drip water at site LA-C2 showed no significant seasonal variations in the measured stable isotope values and elemental ratios, with a mean  $\delta^{18}\text{O}$  value of  $-2.6 \pm 0.1\text{‰}$  (VSMOW) and a mean  $\text{Mg}/\text{Ca}$  ratio of  $0.27 \pm 0.01 (\times 10^{-3})$  (Vieten et al., 2018a, 2018b; Warken, Kuchalski, et al., 2022). The most recent speleothem calcite layer has a  $\delta^{18}\text{O}$  value of  $-3.2\text{‰}$  (VPDB), which is in oxygen isotope equilibrium with the present-day drip water (Coplen, 2007; Tremaine et al., 2011; Vieten, Warken, Winter, Scholz, et al., 2018). The drip site exhibits a high drip rate of about 1 drop per second, with small interannual variability of  $<20\%$ , minimizing potential kinetic effects on the  $\delta^{18}\text{O}$  values of speleothem calcite (Vieten et al., 2018a, 2018b; Warken, Kuchalski, et al., 2022). Over the relatively short length of the record, it is reasonable to assume that the drip characteristics, that is, residence times and lack of seasonal variability in drip water chemistry, did not vary substantially. Thus, the drip site is ideal to study multiannual changes.

## 2.2. Local Climatology

The annual cycle of Puerto Rican rainfall is influenced by moisture convergence and cyclogenesis associated with the expansion and contraction of the western flank of the NASH and determined by the seasonal migration of the ITCZ (Martinez et al., 2019). The summer rainy season is bimodal with an early summer maximum around May, and a late summer peak in August through November (Figures 1b, Hernández Ayala, 2019). The main source of rainfall are the tropical Atlantic Ocean surface waters (Scholl & Murphy, 2014; Vieten et al., 2024). From there, precipitation reaches Puerto Rico as low-pressure systems embedded in easterly convective waves, tropical cyclones and hurricanes, trade wind convergence, and occasional cold fronts from the north-west (Jury

et al., 2007; Scholl & Murphy, 2014). Analyses of rainfall observations only found a weak to moderate influence of decadal North Atlantic teleconnection patterns, such as the Arctic Oscillation or the North Atlantic Oscillation, and only a very minor or even non-significant relationship with ENSO (Hernández Ayala, 2019; Hosannah et al., 2019; Jury et al., 2007; Taylor et al., 2002; Torres-Valcárcel, 2018). Similar studies found that the strongest control of annual and seasonal rainfall amounts can be associated with the AMV (Hernández Ayala, 2019; Stephenson et al., 2014; Taylor et al., 2002).

Rainfall  $\delta^{18}\text{O}$  values at the location of Larga cave as well as the GNIP station San Juan follow the seasonal rainfall pattern with lower  $\delta^{18}\text{O}$  values during the warm season characterized by high amounts of rainfall originating from convective precipitation incl. tropical cyclones and hurricanes. The lowest values occur in rainfall related to hurricanes (Vieten, Warken, Winter, Schröder-Ritzrau, et al., 2018). In contrast, higher  $\delta^{18}\text{O}$  values are recorded during the generally drier winters (Figures 1b, Vieten, Warken, Winter, Schröder-Ritzrau, et al., 2018; Warken et al., 2020). As a consequence, rainfall  $\delta^{18}\text{O}$  values in Puerto Rico have a significant interannual anti-correlation ( $r = -0.73$ ) with rainfall amount, indicating an isotopic “amount effect” of c.  $-0.1\%$  per 100 mm (Vieten et al., 2018a, 2018b, 2024; Warken et al., 2020). This is consistent with results from northeastern and central Puerto Rico (Govender et al., 2013; Scholl & Murphy, 2014; Scholl et al., 2009). Combined with the predominantly singular easterly moisture source from the Caribbean Sea, the  $\delta^{18}\text{O}$  values of precipitation are primarily controlled by rainfall amount in air masses at and upwind of the study area (Vieten et al., 2024; Warken et al., 2020).

### 2.3. $^{230}\text{Th}/\text{U}$ -Dating and Chronology

Seven samples for  $^{230}\text{Th}/\text{U}$ -dating were cut along the growth axis of the stalagmite using a band saw (Figure 1d). Analyses of Th and U isotopes were conducted at the Max Planck Institute for Chemistry (MPIC), Mainz, Germany, using a Nu Plasma multi-collector inductively coupled plasma mass spectrometer (MC-ICPMS). Sample preparation and analytical details of MC-ICPMS measurements of the U and Th isotope ratios are described by Obert et al. (2016) and Yang et al. (2015). Details about the calibration of the mixed U-Th spike are given by Gibert et al. (2016). Age uncertainties are quoted at the  $2\sigma$ -level and do not include half-life uncertainties. The age-depth model (Figure 1c) was constructed using the algorithm StalAge (Scholz & Hoffmann, 2011).

## 2.4. Proxy Analyses

### 2.4.1. Stable Isotopes

Samples were taken via continuous milling along the extension axis of the stalagmite. Oxygen and carbon isotope values were analyzed at a resolution of 0.1 mm up to a depth of 16 mm and at 0.2 mm up to a depth of 52 mm below the top of the stalagmite. Stable isotope measurements were made at the University of Innsbruck. A ThermoFisher Delta V Plus isotope ratio mass spectrometer equipped with a Gasbench II was used (Spötl, 2011). Raw data were calibrated against NBS19, and  $\delta$ -values are reported relative to Vienna Pee Dee Belemnite (VPDB) standard. Long-term precision of the  $\delta^{18}\text{O}$  and  $\delta^{13}\text{C}$  values, estimated as the  $1\sigma$ -standard deviation of replicate analyses, is 0.08 and 0.06‰, respectively (Spötl, 2011; Spötl & Vennemann, 2003).

### 2.4.2. Trace Element Analysis

Samples for Mg/Ca ratios were continuously milled every 0.5 mm along the same trace as sampled for stable isotopes. Mg and Ca were measured on a Horiba Jobin Yvon Ultima 2C inductively coupled plasma optical emission spectrometer at Stony Brook University. Powdered samples were dissolved in 5%  $\text{HNO}_3$  in a volume sufficient to yield a Ca concentration of approximately 80 ppm. The instrument was calibrated using multi-element standards bracketing the expected range of Ca and Mg concentrations (1.6–180 ppm for Ca, and 0.8–10 ppm for Mg). Mg/Ca was corrected for potential instrument drift by running standards after every fifth sample (Schrag, 1999). Reproducibility of the standard and replicate samples in this study is  $\pm 0.06$  and  $\pm 0.08$  mmol/mol, respectively.

## 2.5. Multi-Proxy Coherence

We made the utmost effort to take oxygen isotopes and trace element samples from adjacent positions. To estimate the likelihood that periodic signals in external time series are in-phase with the Mg/Ca and  $\delta^{18}\text{O}$  time series

given age uncertainties, we assess the robustness of the PR-LA-C2 multi-proxy record with a Monte Carlo approach. Accordingly, a large number (10,000) of surrogate annual time series was obtained by interpolating the experimental data of both records to dates resampled from within the dating error according to a uniform distribution. Then, the relative occurrence of cross-wavelet spectra yielding a phase difference between each pair of Mg/Ca and  $\delta^{18}\text{O}$  surrogate records within  $-0.1\pi$  and  $0.1\pi$  was calculated. A value of  $0.1\pi$  is the expectation of occurrence if a phase is purely random; values exceeding this threshold are not determined by chance, yet a higher threshold is sought especially as far as the lowest frequencies in the records are concerned. Wavelet coherence spectra were calculated using the algorithm of Grinsted et al. (2004) and Torrence and Compo (1998). The power of the wavelet coherence spectrum can be interpreted as a measure of the strength of the local correlation between the two time-series in the time-frequency domain.

## 2.6. Complementary Data

We used the precipitation data as available from KNMI Climate Explorer (<https://climexp.knmi.nl>) and NOAA/NCEI (<https://www.ncdc.noaa.gov/gcncm/v2.php>). For calculating the average Puerto Rican precipitation, we used 10 stations closest to Larga Cave that cover at least 25 years (Table S2 in Supporting Information S1). In addition, we used the Paleo Hydrodynamics Data Assimilation product (PHYDA, Steiger et al., 2018), which provides hydroclimate variables over the common era, that is, the past 2 ka. Here, we extracted the Standardized Precipitation-Evapotranspiration Index (SPEI) as an indicator of drought conditions from the two grid boxes covering Puerto Rico and computed their average.

The observed AMV index is the 1856–2017 annual-average time series unsmoothed index from the Kaplan SST V2 calculated at NOAA/ESRL/PSD1 and available at <http://www.esrl.noaa.gov/psd/data/timeseries/AMO>. The observed PDV index is the 1854–2022 annual-average time series of the NCEI PDO index based on NOAA's extended reconstruction of SSTs (ERSST V5) and available at <https://www.ncei.noaa.gov/access/monitoring/pdo/>. Gridded SST observational data for the period 1870–2019 were obtained from the Hadley Center Sea Ice and SST data set (HadISST1, Rayner et al., 2003) and used to calculate Caribbean SSTs (spatial average over the domain 80–50°W and 9–23°N) and Pacific-Atlantic SST gradient (Atlantic minus Pacific) following Bhattacharya and Coats (2020).

Variations in solar forcing are expressed in terms of total solar irradiance (TSI) changes (Figures 2a and 2b). In order to account for uncertainties in TSI reconstructions, two time series are considered: (a) the TSI obtained from the semi-empirical SATIRE model, which is among the recommended time series for the Coupled Model Intercomparison Project Phase 6 (Matthes et al., 2017); (b) the upscaled TSI time series to match a variability (max-min) of 0.25% of the standard TSI value of 1367 W/m<sup>2</sup> used in the solar forcing Millennium COSMOS experiment based on the ECHAM5/MPIOM Earth system model (Jungclauss, 2008; Jungclauss et al., 2010), referred to as “Krivova.”

Volcanic forcing estimates are derived from numerical paleoclimate simulations following Winter et al. (2015). Specifically, volcanic forcing estimates for CCSM4 are derived from the full-forcing last-millennium simulation available in the Coupled Model Intercomparison Project 5 repository (Landrum et al., 2013), a volcanic-forcing only last-millennium simulation is considered for the COSMOS Earth system model (Jungclauss et al., 2010), and a natural forcing (volcanic and solar) last-millennium simulation is used for the Bergen Climate Model (BCM, Otterå et al., 2010). Different reconstructions of aerosol optical properties for volcanic forcing were used, and the reader is referred to Winter et al. (2015) for further details. Cumulative volcanic forcing is obtained by cumulatively adding through time the forcing of each volcanic event within “volcanic clusters,” where each cluster is defined as a sequence of strong volcanic events occurring within temporal intervals of 40 years or less.

## 3. Results and Discussion

### 3.1. Speleothem PR-LA-C2 Multi-Proxy Record

#### 3.1.1. Chronology

<sup>230</sup>Th/U-dating (Figure 1c) shows that stalagmite PR-LA-C2 grew continuously during the last 500 years (1500 CE-present). The U content is between 0.38 and 0.83 μg/g, and for most samples the (<sup>230</sup>Th/<sup>232</sup>Th) activity ratios are high (Table S1 in Supporting Information S1). However, the detrital <sup>232</sup>Th content is significant, even for comparably clean samples from Larga Cave (Warken et al., 2020), and also for stalagmites from other caves in

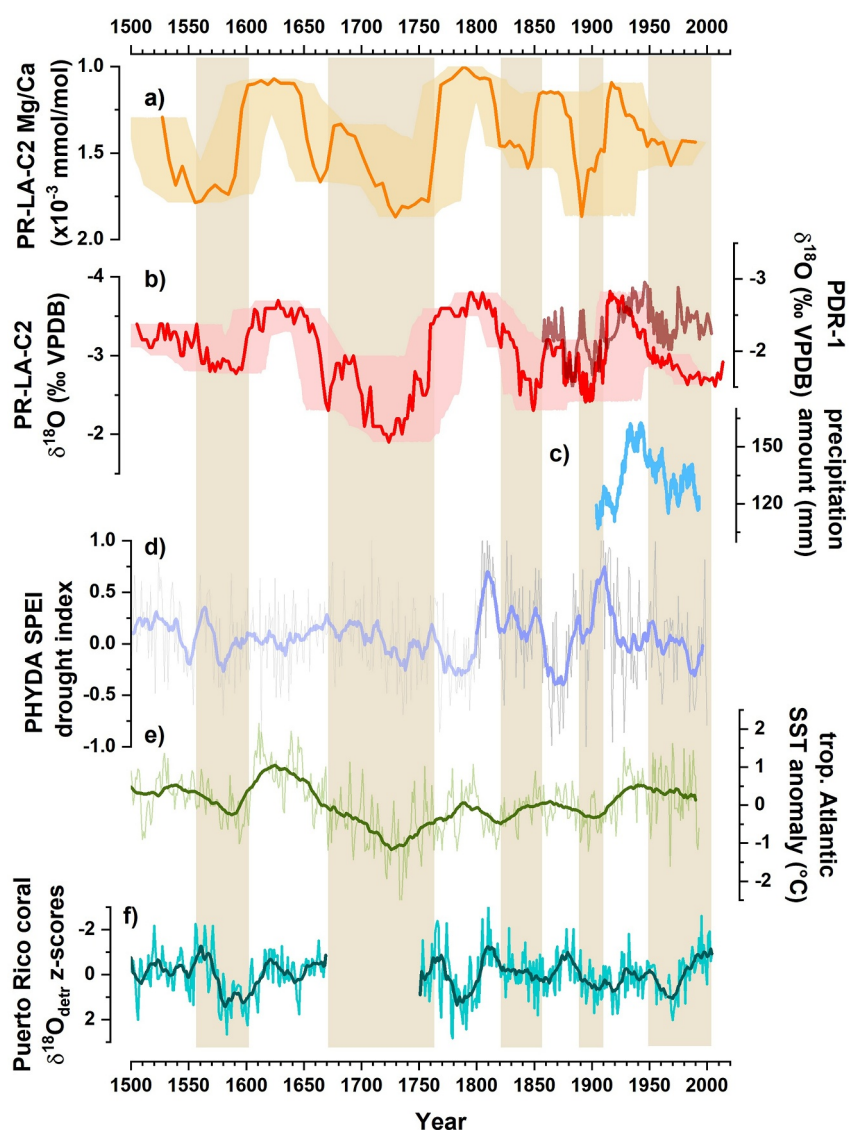


**Figure 2.** Puerto Rico Larga cave proxy records compared to regional precipitation and sea-surface temperature (SST) records. All panels are oriented to reflect warmer/wetter conditions toward the top, and colder/drier conditions toward the bottom. (a) PR-LA-C2 Mg/Ca record with uncertainty envelope (shading); (b) PR-LA-C2  $\delta^{18}\text{O}$  record with uncertainty (shading) as well as the Perdida Cave (PDR-1)  $\delta^{18}\text{O}$  speleothem record (Winter et al., 2011). Note that due to relatively poor resolution and age control before c. 1850 AD, only the modern part of the PDR-1 record is shown; (c) Puerto Rican multi-station mean monthly precipitation amount (see text for more details); (d) PHYDA Standardized Precipitation-Evapotranspiration Index drought index (Steiger et al., 2018). Before c. 1800 AD, the data is shown in lighter colors because the data assimilation product is not well constrained in this grid box; (e) tropical Atlantic SST anomaly as derived from the detrended and normalized sclerosponge-based SST reconstruction of Waite et al. (2020); (f) Puerto Rico coral detrended  $\delta^{18}\text{O}$  values (Kilbourne et al., 2008, 2014) converted to z-scores as an indicator of SST anomalies. Vertical brown bars indicate decades of relatively dry conditions on Puerto Rico.

Puerto Rico (Rivera-Collazo et al., 2015; Vieten et al., 2024) and other Caribbean locations (e.g., Fensterer et al., 2010; Steidle et al., 2021). Therefore, we regard the bulk Earth detrital ( $^{230}\text{Th}/^{232}\text{Th}$ ) activity ratio of 0.8 as inappropriate to account for initial  $^{230}\text{Th}$  in stalagmite PR-LA-C2. To bring all ages in stratigraphic order with the two clean ages at 0.5 and 3.2 cm dft, we assumed a ( $^{230}\text{Th}/^{232}\text{Th}$ ) activity ratio of  $61.1 \pm 61.1$  and secular equilibrium for the detritus to correct the activity ratios and ages for detrital  $^{230}\text{Th}$ . This ( $^{230}\text{Th}/^{232}\text{Th}$ ) value is consistent within uncertainty with other studies from Larga Cave and this region (e.g., Fensterer et al., 2010; Rivera-Collazo et al., 2015; Steidle et al., 2021; Vieten et al., 2024; Warken et al., 2020). However, due to the high

( $^{230}\text{Th}/^{232}\text{Th}$ ) ratios of PR-LA-C2, the correction is still small resulting in uncertainties of the corrected, individual ages between 10 and 100 years (Table S1 in Supporting Information S1). The uncertainty of the resulting age-depth model obtained by StalAge ranges from 10 to 50 years over most parts of the record. The average growth rate of PR-LA-C2 is more than 100  $\mu\text{m}/\text{a}$ , which results in a close to annual resolution of the stable isotope values, and around 5 years for Mg/Ca.

### 3.1.2. Proxy Interpretation

Figures 2a and 2b illustrate the temporal evolution of the PR-LA-C2 multiproxy record during the past five centuries. Monitoring of the drip site of PR-LA-C2 shows relatively constant drip rates, and it can be assumed that fracture flow is not dominant at this site (Vieten et al., 2018a, 2018b; Warken, Kuchalski, et al., 2022). As a consequence, drip water  $\delta^{18}\text{O}$  values show only little variability and reflect the annual mean  $\delta^{18}\text{O}$  value of precipitation (Vieten et al., 2018a, 2018b). Hence, on an interannual scale, speleothem  $\delta^{18}\text{O}$  values are expected to reflect changes in Puerto Rican rainfall amount (Vieten et al., 2024; Warken et al., 2020). This is supported by the good co-variance within dating uncertainties of the PR-LA-C2  $\delta^{18}\text{O}$  record with the stalagmite  $\delta^{18}\text{O}$  data from Perdida Cave (Winter et al., 2011), which provides a comparable resolution as our record back until c. 1850 AD (Figure 2b).

For some drip sites in Larga cave, an influence of  $\delta^{18}\text{O}$ -depleted TC precipitation cannot be excluded (Vieten, Warken, Winter, Schröder-Ritzrau, et al., 2018). Even though no direct influence was detectable at drip site C2, we explore a potential influence of TC-related rainfall on the  $\delta^{18}\text{O}$  signature of speleothem PR-LA-C2. To this end, we compare our record with historical TC counts from the HURDAT2 database (Landsea & Franklin, 2013) as well as regional, proxy-based reconstructions (e.g., Burn & Palmer, 2015; Nyberg et al., 2007). This comparison reveals no clear pattern (Figure 3), which could be due to both dating uncertainties and archive resolution. Moreover, sedimentary archives do not necessarily record high precipitation events, and tropical cyclones and depressions with comparably weak wind speeds or storm surges can still bring a considerable amount of  $\delta^{18}\text{O}$  depleted rainfall (e.g., Govender et al., 2013; Warken, Kuchalski, et al., 2022). Interestingly, our record shares a similar pattern with a recent study combining sedimentary paleo-hurricane records and a statistical reconstruction of hurricane activity dependent on SSTs (Yang et al., 2024) (Figure 3). Taking dating uncertainties into account, periods of lower speleothem  $\delta^{18}\text{O}$  values appear to coincide with times of higher statistical probability of hurricane occurrence associated with warmer SSTs (Yang et al., 2024). We interpret this common pattern such that warmer SSTs generally support enhanced convection and cyclogenesis, from tropical waves, depressions, tropical storms, and hurricanes, which altogether result in higher rainfall amounts affecting Puerto Rico. Nevertheless, although individual events cannot be resolved by our record, the results of Yang et al. (2024) generally support our assessment that lower speleothem  $\delta^{18}\text{O}$  values reflect higher convective rainfall amount.

The pronounced co-variability of the PR-LA-C2 proxies (Figures S1 and S2 in Supporting Information S1) provides additional support for a strong underlying hydroclimatic control via the “amount effect” on speleothem  $\delta^{18}\text{O}$  values, and Mg/Ca ( $\delta^{13}\text{C}$ ) values reflecting changes in prior calcite precipitation (PCP) and residence time (Johnson et al., 2006), similar to what has been observed for other stalagmites from Larga cave and other sites on Puerto Rico (Vieten et al., 2024; Warken et al., 2020). These processes are typically enhanced during drier periods with reduced recharge, and result in an increase in the Mg/Ca ( $\delta^{13}\text{C}$ ) values of the solution, and, subsequently, the speleothem (Fairchild et al., 2000; Johnson et al., 2006). Drier phases in Puerto Rico are mainly associated with a reduced contribution of convective summer rainfall to the drip water reservoir, which shifts the mean annual  $\delta^{18}\text{O}$  value of the infiltrating water toward higher values (Vieten et al., 2024). Hence, in a setting like Larga Cave, site-specific karst-hydrological effects and PCP are expected to accompany or even exacerbate the amount effect on rainfall  $\delta^{18}\text{O}$  values (Deininger et al., 2021; Warken et al., 2020). This is, for example, visible in the temporal evolution of the proxy data. The stable proxy values during the dry and wet phases and the rapid transitions in between suggest that the underlying process may follow a non-linear bi-stable regime rather than an oscillatory behavior. A potential explanation for this observed pattern may be non-linear hydrological responses in the karst system (Priestley et al., 2023; Treble et al., 2022). In summary, the strong correlations between speleothem  $\delta^{18}\text{O}$ ,  $\delta^{13}\text{C}$ , and Mg/Ca values suggest a non-negligible role of in-cave processes, such as PCP. However, the comparison with instrumental data also justifies the interpretation of the speleothem multi-proxy record as a robust indicator of local water balance related to rainfall amount (Figure 2c). In addition, the speleothem proxies robustly reflect the transition from drier to wetter conditions during the early twentieth century, with the wettest phase around the 1940s (within dating uncertainties). Likewise, the subsequent progressive drying trend is recorded by

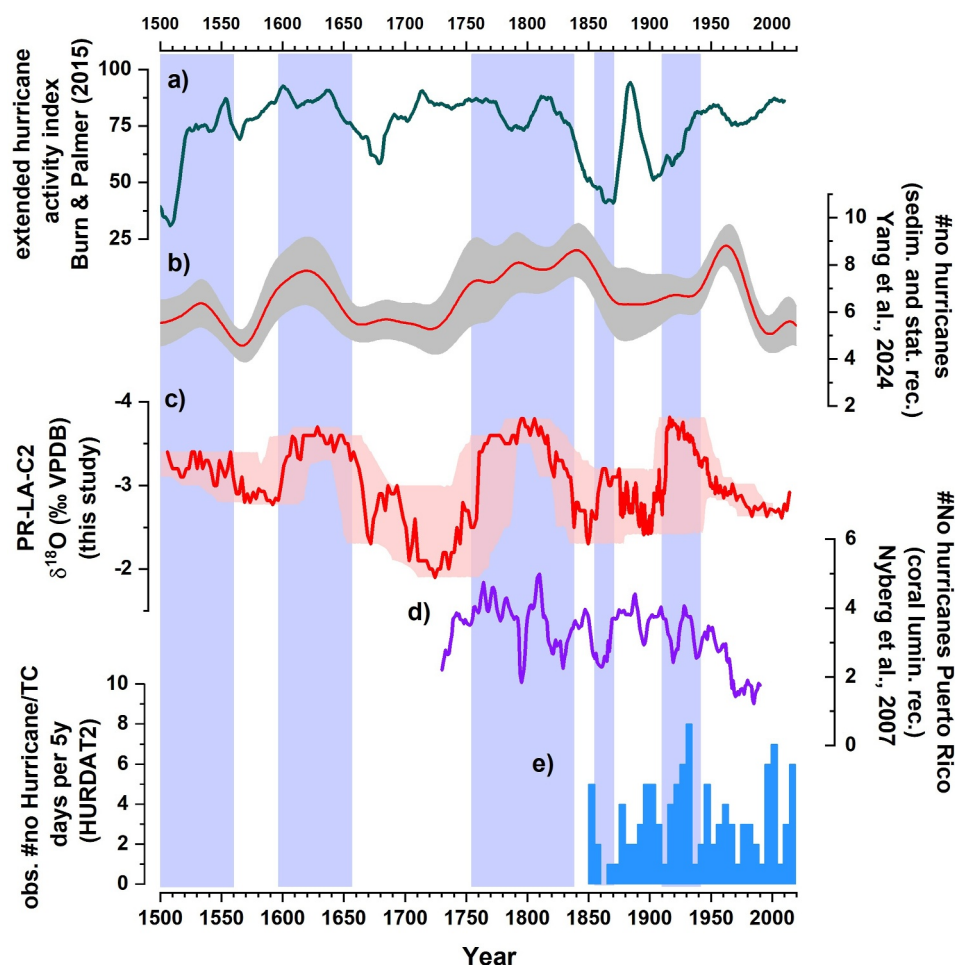


**Figure 3.** Comparison of several tropical cyclone (TC) reconstructions. From top to bottom: (a) Atlantic hurricane activity index reconstruction (Burn & Palmer, 2015); (b) tropical Atlantic hurricane activity reconstruction (Yang et al., 2024); (c) PR-LA-C2  $\delta^{18}\text{O}$  record (this study); (d) Puerto Rican hurricane activity reconstructed from coral luminescence records from Puerto Rico (Nyberg et al., 2007); (e) historical counts of hurricane/tropical cyclones per 5 years in Puerto Rico as archived in the HURDAT2 database (Landsea & Franklin, 2013). Blue bars indicate times of low speleothem  $\delta^{18}\text{O}$  values indicative of enhanced convective activity and higher rainfall amounts.

less negative speleothem  $\delta^{18}\text{O}$  values. The lack of meteorological data precludes inferences beyond the instrumental period, but a comparison with the reconstructed PHYDA SPEI drought index (Steiger et al., 2018) provides further support for the interpretation of our record for the period up to c. 1800 AD (Figure 2b). Prior to that, the PHYDA data assimilation product is largely unconstrained in the Caribbean area due to a lack of hydroclimatically sensitive data in the region (Steiger et al., 2018).

In summary, this discussion shows that the PR-LA-C2 record captured the large-scale rainfall amount signal and not only local conditions related to runoff or in-cave processes (Figure 2d). The previous discussion of a potential influence of  $\delta^{18}\text{O}$ -depleted TC rainfall also justifies the interpretation of speleothem  $\delta^{18}\text{O}$  values as recorders of rainfall amount related to convective activity. Still, due to dating uncertainties and potentially underlying non-linear effects, we refrain from quantitative inferences on rainfall amount from the speleothem proxies and focus on the general patterns visible on multi-decadal to centennial timescales.

### 3.1.3. Temporal Evolution

The resulting speleothem time series is largely dominated by the alternation of multidecadal-to-centennial periods of anomalously dry and wet conditions separated by decadal-scale transitions. The most recent periods include a wet interval peaking in the first half of the twentieth century and progressively drier conditions until the 1980/90s



(Figure 2). Within dating uncertainties, this general feature of the PR-LA-C2 multiproxy record corresponds well to the evolution of Puerto Rican summer rainfall from meteorological observations (Figure 2c), as well as a previous speleothem-derived rainfall reconstruction (Winter et al., 2011). The pronounced multidecadal to centennial scale variability is further highlighted by the very energetic but broad spectral peak around the 100-year periodicity observed in the energy spectra of the surrogate series of both Mg/Ca and  $\delta^{18}\text{O}$  values, with the significance envelope highlighting the multidecadal portion of the spectrum in the former and the multi-centennial portion in the latter (Figures S2 and S6 in Supporting Information S1). Accounting for age uncertainty (shading in Figures 2a and 2b), the most prominent multidecadal to centennial wet phases observed in both records occurred between c. 1600 and 1650, 1760 to 1830, and 1915 to 1940 CE, whereas a pronounced consistent dry phase was identified between 1700 and 1750 CE.

### 3.2. Link of Puerto Rican Precipitation to Atlantic SSTs and AMV

Warmer surface temperatures of the tropical Atlantic Ocean sustain enhanced convection in the moisture source locations of Puerto Rican precipitation, and hence are interpreted to cause more rainfall at the site, in particular during the wet summer season (Stephenson et al., 2014; Wang et al., 2006; Yang et al., 2024). Correlation analysis confirms that rainfall amount in Puerto Rico is linked to SST anomalies (SSTA) in the tropical Atlantic with  $r = 0.48$  ( $p < 0.01$ ) (Figures S3 to S5 in Supporting Information S1). This is also seen in the wavelet coherence, with a clear co-phase and a shift in periodicity of the two parameters (Figure S4 in Supporting Information S1), as well as spatial correlation with basin wide SSTs (Figure S5 in Supporting Information S1). Prior to the twentieth century, this observation is supported by similar variations of the speleothem proxies and tropical Atlantic SST-sensitive tropical coral  $\delta^{18}\text{O}$  data (Figure 2f, Kilbourne et al., 2008, 2014), reconstructed SSTAs from a sclerosponge-based record from the Bahamas (Figure 2e, Waite et al., 2020), as well as SST-related cyclogenesis (Figure 3b, Yang et al., 2024). This shows that the multidecadal wet phases in Puerto Rico were associated with relatively warm SSTs and vice versa (Figure 2) confirming that Atlantic SST changes have been a dominant precursor of Puerto Rican precipitation since c. 1500 AD.

The apparent regime bi-stability in the reconstructed Puerto Rican rainfall contrasts with the more oscillatory behavior of regional SST/SSTAs. A possible process entails an on-off dependency of deep atmospheric convection on local SSTs, such that deep convection is only activated above a certain SST threshold (Evans & Webster, 2014; Johnson & Xie, 2010; Winter et al., 2020). Accordingly, the sharp transitions detected in the PR-LA-C2  $\delta^{18}\text{O}$  record may reflect gradual SST warmings inducing sharp transitions in the frequency and intensity of deep convection and cyclogenesis once such a threshold is surpassed, hence rapidly enhancing the total amount of rainfall in the catchment of the cave. This is supported by the similarity of the Larga cave speleothem record with the statistical SST-based reconstruction of hurricane activity by Yang et al. (2024). However, another plausible explanation for this threshold behavior could be site-specific, and related to non-linear karst hydrological effects, such as changes in the contribution from different flow paths and reservoirs (Treble et al., 2022, see Section 3.1.2).

Reconstructions across the western tropical Atlantic have shown that Caribbean and western tropical Atlantic SSTs varied in concert with the AMV, that is, basin-wide, quasiperiodic oscillations of North Atlantic SSTs (Vásquez-Bedoya et al., 2012; Waite et al., 2020; Wang et al., 2006). Consequently, the multidecadal to centennial fluctuations in the multiproxy PR-LA-C2 record also appear related to alternating phases of the AMV, with warm AMV being associated with wetter conditions and vice versa (Figures 4c, 4d, and 4f). A strong interdecadal connection between Puerto Rican rainfall and AMV also emerges from the observational records of both variables (Figures 2e and 2f). This manifests in a strong correlation between Puerto Rican rainfall amount and the observed AMV index ( $r = 0.59$   $p < 0.01$ , Figure S3 in Supporting Information S1), and a robust wavelet phase at interdecadal time scales (Figure S4 in Supporting Information S1). Wavelet coherence between the PR-LA-C2  $\delta^{18}\text{O}$  record, the SST reconstruction by Waite et al. (2020), and the AMV reconstruction by Svendsen et al. (2014) indicate a synchronous pattern of AMV, Caribbean SSTs and Puerto Rican precipitation since c. 1750 AD (Figure 5). The increasing spread in the existing AMV reconstructions prior to ca. 1750 AD makes further analysis for earlier times challenging (Hernández et al., 2020).

In summary, this analysis provides evidence for the previously hypothesized mechanism linking AMV, Caribbean SSTs and regional rainfall (Fensterer et al., 2012; Wang et al., 2006). Within the AMV framework, basin-scale ocean dynamics in the North Atlantic Ocean modulate Caribbean SSTs (Vásquez-Bedoya et al., 2012),

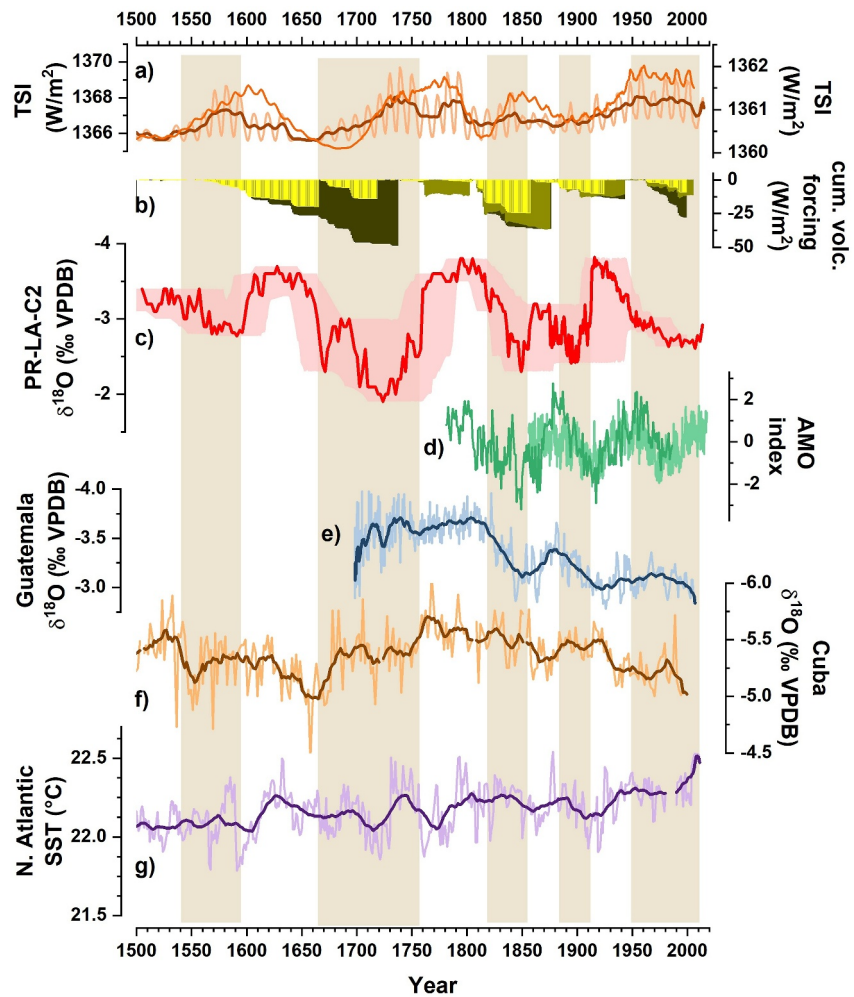


**Figure 4.** Comparison of the Larga cave proxy record with other regional records and associated forcing mechanisms. (a) Time series of reconstructed total solar irradiance (Jungclauss, 2008; Jungclauss et al., 2010; Matthes et al., 2017), (b) time series of cumulative volcanic forcing from paleoclimate simulations (black: BCM; brown: CCSM4; yellow: COSMOS; after Winter et al., 2015), (c) PR-LA-C2  $\delta^{18}\text{O}$  record with uncertainty as surrogate envelope (shading), (d) standardized AMO time series including reconstructions from Svendsen et al. (2014) (dark green) and observations (light green). (e) Guatemala Xibalba speleothem  $\delta^{18}\text{O}$  values (Winter et al., 2015), (f) Cuba speleothem CG  $\delta^{18}\text{O}$  values (Fensterer et al., 2012), (g) North Atlantic sea-surface temperature reconstruction (Lapointe et al., 2020).

which in turn control the intensity of local atmospheric convective activity, and hence directly impact regional precipitation (Wang et al., 2006; Winter et al., 2020). Dynamics linked to anomalously warm Caribbean SSTs under a positive AMV and the associated development of a near-surface negative pressure anomaly in the western tropical Atlantic and the Caribbean low-level jet core region provide an additional feedback mechanism to support a connection between AMV and Caribbean rainfall (Taylor et al., 2011).

### 3.3. Regional Comparison—Common Signals and Discrepancies

Although many records from the common era documenting a multidecadal to centennial variability in precipitation and/or SSTs, a detailed inspection of the regional records reveals some disagreement concerning the timing of events as well as dominant periodicities. In the PR-LA-C2 record, the shorter, decadal-to multidecadal-scale mode of variability is distinctly suppressed relative to other regional records of precipitation and SST variability. For example, a Puerto Rican coral  $\delta^{18}\text{O}$ -SST history spanning the last 250 years also displays clear decadal to multidecadal scale variability (Kilbourne et al., 2008), but a multidecadal to centennial mode is not apparent until the coral  $\delta^{18}\text{O}$  data are detrended and filtered (Figure 2f). The Puerto Rican speleothem and coral data show

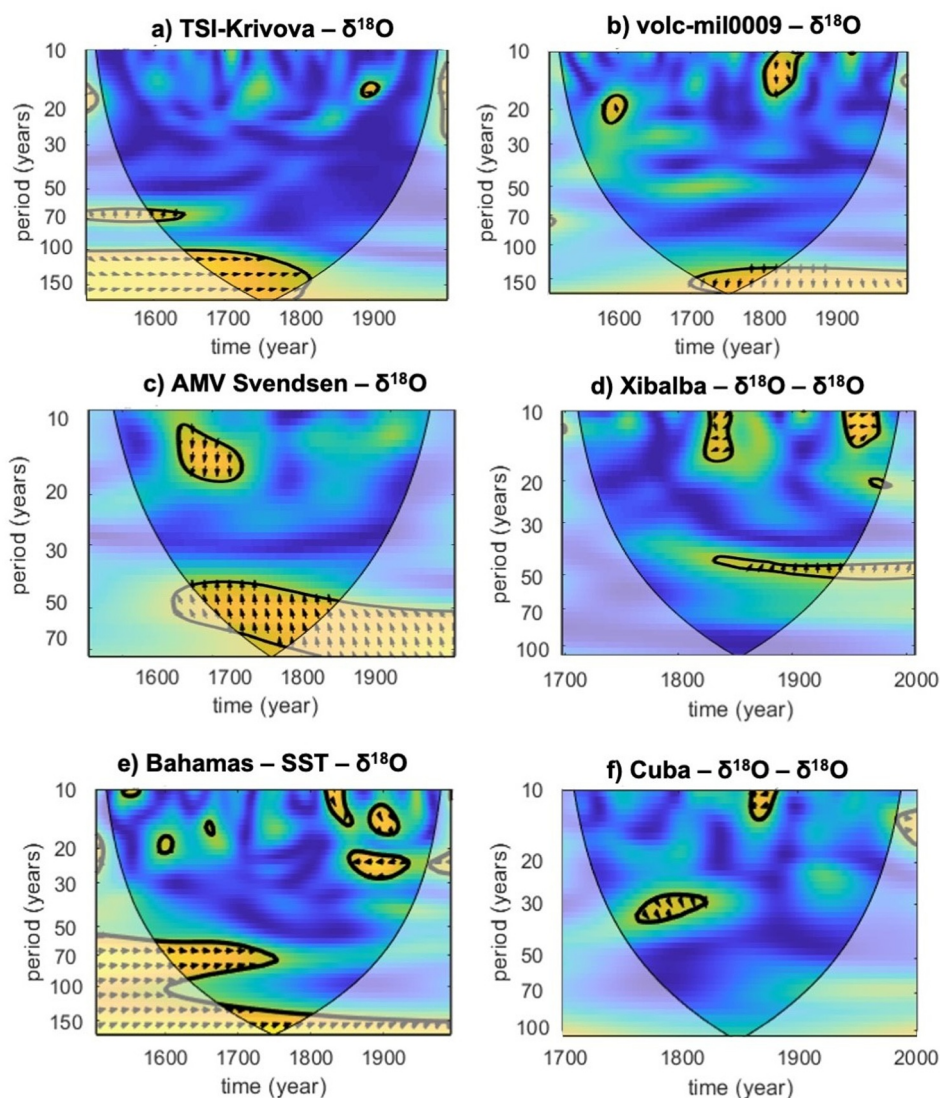


**Figure 5.** Wavelet coherences between the PR-LA-C2  $\delta^{18}\text{O}$  record, potential forcing factors of Caribbean precipitation variability, and other regional records. Panels show analysis with (a) solar activity (Jungclauss, 2008), (b) volcanic activity (simulated top-of-atmosphere forcing from COSMOS (Jungclauss et al., 2010), (c) AMV (reconstruction by Svendsen et al., 2014), (d) the linearly detrended GU-Xi-1  $\delta^{18}\text{O}$  record (Winter et al., 2015), (e) sea-surface temperature reconstruction from Lee Stocking Island, Bahamas (Waite et al., 2020), as well as the detrended CG  $\delta^{18}\text{O}$  record from Cuba (Fensterer et al., 2012). All  $\delta^{18}\text{O}$  values are multiplied by  $-1$  for this analysis. The color shading illustrates the local amplitude of the wavelet coherence spectrum, from small (blue) to large (yellow). Thick contours identify the 5% significance level. Arrows identify the phases (eastward-pointed arrows identify co-phase, the PR-CL-C2  $\delta^{18}\text{O}$  record leads for anticlockwise rotation from the co-phase axis). The shaded region indicates where edge effects occur.

similar patterns to the AMV index (Figures 2c, 2d, and 2f) for most of the interval of overlap, although the coral data contain a peak in multidecadal variability post-1970 that is not apparent in the speleothem data.

Similarly, a speleothem  $\delta^{18}\text{O}$  record from Cuba (Fensterer et al., 2012) exhibits clear decadal-scale variability but again lacks distinctive multidecadal to centennial-scale variability (Figures 4e and 5e). Puerto Rico coral SSTs increase over the last 250 years, but the Puerto Rican and Cuban speleothem precipitation reconstructions do not show such a warming trend, suggesting that absolute regional SSTs are not the only control on precipitation over this time interval, an assertion further supported by a three century-long increase in both tropical and larger-North Atlantic reconstructed SSTs (Figures 4f and 4g; Lapointe et al., 2020; Waite et al., 2020) that are not matched by any of the regional speleothem precipitation records (Figures 4a–4c and 4e).

A shorter record that shows pronounced multidecadal-to-centennial variations similar to the PR-LA-C2 multiproxy record (Figures 3a and 3b) is the GU-Xi-1  $\delta^{18}\text{O}$  record of Yucatán Peninsula precipitation covering the past three centuries (Winter et al., 2015) (Figure 3e). This record also displays recurrent  $\delta^{18}\text{O}$  minima around  $-4\text{‰}$  and a prolonged wet phase until the early nineteenth century followed by a pronounced drying trend until present. These features in GU-XI-1 contrast with the PR-LA-C2 record, which is dominated by multidecadal-to-centennial variability rather than multi-centennial features. Nonetheless, once the Yucatán Peninsula record is linearly detrended, the wavelet coherence spectra between  $\delta^{18}\text{O}$  records from both locations indicate common multidecadal variability around the 40 to 50-year time scale since about 1800 CE (Figure 4). Within uncertainties, the Puerto Rican and Yucatán Peninsula records are synchronous.

While our analysis shows a clear connection between Puerto Rican rainfall amount and tropical Atlantic SSTA, the regional comparison recommends caution about general inferences on potential large-scale expressions of the AMV in the Caribbean realm. One reason for the observed discrepancies may be archive-specific issues, such as dating uncertainties, internal noise, memory or smoothing of the individual records, or heterogeneous proxy sensitivity. Additional, replicated, high resolution paleoclimate reconstructions from the wider region covering a longer time period could support or reject some of these processes. On the other hand, the regional heterogeneity suggests superimposing influences on regional hydroclimate. A changing Pacific-Atlantic inter-basin SSTA gradient may modulate the Walker circulation and in turn change the tropical convective activity over the tropical Pacific and Atlantic (e.g., Bhattacharya & Coats, 2020; Kim et al., 2020). We note that the correlation of instrumental Puerto Rican rainfall amount with the Pacific-Atlantic inter-basin SST gradient is insignificant independent of the chosen period of the year, whereas significant yet comparably weak for the PDO index ( $r = 0.22$ ,  $p = 0.07$  for annual-average values, and  $r = 0.30$ ,  $p = 0.01$  for winter values). However, while Caribbean SSTs are part of the AMV pattern, Pacific and Atlantic decadal and multidecadal patterns are known to be not independent, and precipitation resembles the PDO index during certain periods (Figure S2 in Supporting Information S1). Therefore, we cannot fully rule out a preconditioning role from interdecadal Pacific SST changes.

### 3.4. Potential Forcing Mechanisms

Various processes have been discussed as potential forcing mechanisms of Caribbean precipitation on the multidecadal to centennial scale. Changes in natural forcing, such as solar activity and energetic volcanic eruptions, have been suggested as major drivers of (hydro)climate variability during the past millennium (e.g., PAGES Consortium, 2017; Wang et al., 2017). In the Caribbean paleoclimate record, imprints of solar cycles throughout the Holocene period have been documented by various studies (Black et al., 1999; Burn & Palmer, 2014; Haase-Schramm et al., 2003; Hodell et al., 2001; Pollock et al., 2016; Ridley et al., 2015; Smirnov et al., 2017; Waite et al., 2020; Warken et al., 2021; Winter et al., 2015). The multiproxy PR-LA-C2 record contains significant signals related to natural forcing (Figure 5 and Figure S1 in Supporting Information S1). Reconstructions of both solar and volcanic forcing are affected by substantial uncertainties (Figures 2a and 2b) (e.g., Zanchettin, Bothe, Rubino, & Jungclaus, 2016), and we therefore provide only the most prominent results. Grand solar changes appear to have been in phase with  $\delta^{18}\text{O}$  fluctuations in PR-LA-C2 until around 1800 CE (Figure 5a). There is a tendency toward drier conditions during the Maunder Minimum of solar activity in the second half of the seventeenth century and the early eighteenth century, followed by wetter conditions under increased solar activity (Figure 2).

Wavelet coherence indicates that volcanic forcing is significantly linked with centennial-scale  $\delta^{18}\text{O}$  fluctuations in PR-LA-C2 since around 1700 CE, with a delay of a couple of decades in the response seen as a phase-lag between signals by  $90^\circ$  (Figure 5b). Such a delay can be interpreted as a cumulative hydroclimate response to clusters of large volcanic eruptions, most prominently the early nineteenth century cluster with the 1809 unknown and 1815 Tambora eruptions, the late nineteenth century cluster including the 1883 Krakatau and Santa Maria 1900 eruptions, and the twentieth century cluster with the 1963 Agung, 1982 El Chichón and 1991 Pinatubo eruptions (Figure 2b). The coherence spectrum obtained using cumulative volcanic forcing does not display this centennial-scale connection (not shown), suggesting that this reflects dynamical than merely direct radiative responses.

The coherence detected in the eighteenth century, when there was no major eruption or volcanic cluster, is interpreted to reflect the connection between lack of volcanic activity, warmer SSTs, and thus wetter conditions in

Puerto Rico. This agrees with the observation by Ridley et al. (2015), who suggested modulation of Caribbean SSTs as a possible explanation for the observed link between volcanic forcing and Mesoamerican precipitation (Ridley et al., 2015). Solar cycles are hypothesized to modulate SSTs of the North Atlantic Ocean via combined atmospheric and ocean circulation effects (Bond et al., 2001; Jiang et al., 2015; Marchitto et al., 2010; Moffa-Sánchez et al., 2014). Weak (strong) solar activity could have induced a concomitant cooling (warming) in the tropical Atlantic as well as changes in the Hadley circulation, that is, enhanced (reduced) trade wind variability (Black et al., 1999). In addition, it has been suggested that changes in solar irradiance could influence the tropical Pacific via the so-called “ocean dynamical thermostat” response, because negative (positive) radiative forcing results in a warming (cooling) of the eastern tropical Pacific, and hence more El Niño-like (more La Niña-like) conditions (Clement et al., 1996; Mann et al., 2005; Marchitto et al., 2010). Both effects would explain drier (wetter) conditions associated with negative (positive) radiative forcing in the Caribbean (Burn & Palmer, 2014).

The AMV, to which North Atlantic and Caribbean SSTs are integrally linked, is at least partly a natural phenomenon, as recent analyses of observations, re-analyses and climate model simulations suggest (Birkel et al., 2018; Mann et al., 2020; Wang et al., 2017). Recent research has therefore attempted to disentangle the AMV evolution during the past millennium into its externally forced and intrinsic components (Fang et al., 2021; Wang et al., 2017). However, a model study based on multimillennial unperturbed preindustrial and Holocene transient simulations, including and excluding volcanic forcing, demonstrated that individual events of strong AMV fluctuations can display significantly different anomalous spatial patterns, especially over the subpolar North Atlantic and the tropics (Zanchettin et al., 2023). This also poses the question of which aspect of the AMV is predominantly captured by individual study locations and different proxies (Hernández et al., 2020). Hence, the proposed relation between volcanic eruptions, AMV, and tropical precipitation over periods of more than a few centuries is uncertain because of the limited temporal coverage of these studies considering the known non-stationarity of teleconnections and dependency of responses on initial conditions and mean climate state (e.g., Swingedouw et al., 2015; Zanchettin et al., 2013). Accordingly, the reconstructed Caribbean SST variability during the past 600 years from Lee Stocking Island, Bahamas, entails periods when the AMV signal can be traced back to volcanic activity and periods when it was incoherent with external forcing, thereby suggesting predominance of intrinsic (or endogenous) climate variability (Waite et al., 2020; Yang et al., 2024).

#### 4. Conclusions

The multiproxy PR-LA-C2 record illustrates the evolution of northeastern Caribbean rainfall during the past five centuries, which we posit is dominated by the alternation between multidecadal to centennial dry and wet phases potentially linked to changes in natural forcing, such as solar and/or volcanic activity. The record shows that the rainfall regime is primarily controlled by local atmospheric convection driven by SST changes in the tropical sector of the North Atlantic. The intertwining between Caribbean SST variability and the basin-scale changes associated with the AMV may explain the dominance of multidecadal to centennial fluctuations in the spectrum of Caribbean rainfall and could provide a framework for its interpretation as a response to natural forcing.

Nonetheless, several questions arise from our results. While a robust synchronicity between PR-LA-C2 and AMV records appears to exist back to the eighteenth century, the diversity of AMV characteristics simulated by coupled climate models (e.g., Mann et al., 2020; Zanchettin et al., 2014) and the substantial variability through time of the AMV fingerprint on tropical SSTs in climate model simulations (Zanchettin et al., 2023) means that PR-LA-C2 record may not be a straightforward AMV proxy. Still, the connection between Caribbean precipitation and Caribbean SSTs, and hence the western tropical branch of the AMV, and the discussed link with solar and volcanic forcing provide support that the AMV pattern could be linked to external radiative forcing (Fang et al., 2021; Klavans et al., 2022; Waite et al., 2020).

A further open question is how the warm-wet and cold-dry scenarios observed in our and other record compare with expected changes under future climate scenarios. Most models indicate a drying over the Caribbean under global warming (Khalyani et al., 2016; Neelin et al., 2006), which is contrary to the natural mechanisms illustrated here. It is arguable that other possible climatic patterns beyond the one linking AMV, Caribbean SST, local atmospheric convection and cyclogenesis incl. hurricanes with rainfall amount, may become dominant as warming progresses. Among these are meridional shifts in the positions of the Hadley Cell and especially the ITCZ and the related tropical rainfall bands. Nonetheless, observations of Puerto Rican rainfall show no

significant century-scale trends (Jones et al., 2016), and the natural variability illustrated in this paper may therefore remain dominant in the upcoming decades.

## Data Availability Statement

Data is accessible at Vieten et al. (2023).

## Acknowledgments

We appreciate the continuous support from the University of Puerto Rico and we thank Yelitsa González for providing isotopic measurements, and we are grateful to Wilson Ramírez Martínez. In addition, we thank and miss Felipe Rodríguez-Morales for long-term support. We acknowledge support from the National Science Foundation Grant ATM-1003502. DS is thankful for funding from the German Research Foundation (DFG SCHO 1274/9-1 and SCHO 1274/11-1) and K.P. Jochum, M.O. Andreae, and G.H. Haug for support. SW acknowledges the support and fruitful discussions with N. Frank and A. Schröder-Ritzrau, as well as support from Heidelberg University via the Olympia Morata program. Open Access funding enabled and organized by Projekt DEAL.

## References

- Asmerom, Y., Baldini, J. U., Pruffer, K. M., Polyak, V. J., Ridley, H. E., Aquino, V. V., et al. (2020). Intertropical convergence zone variability in the Neotropics during the Common Era. *Science Advances*, 6(7), eaax3644. <https://doi.org/10.1126/sciadv.aax3644>
- Bhattacharya, T., & Coats, S. (2020). Atlantic-Pacific gradients drive last millennium hydroclimate variability in Mesoamerica. *Geophysical Research Letters*, 47(13), e2020GL088061. <https://doi.org/10.1029/2020gl088061>
- Birkel, S. D., Mayewski, P. A., Maasch, K. A., Kurbatov, A. V., & Lyon, B. (2018). Evidence for a volcanic underpinning of the Atlantic multidecadal oscillation. *NPJ Climate and Atmospheric Science*, 1(1), 1–7. <https://doi.org/10.1038/s41612-018-0036-6>
- Black, D. E., Peterson, L. C., Overpeck, J. T., Kaplan, A., Evans, M. N., & Kashgarian, M. (1999). Eight centuries of north Atlantic Ocean atmosphere variability. *Science*, 286(5445), 1709–1713. <https://doi.org/10.1126/science.286.5445.1709>
- Bond, G., Kromer, B., Beer, J., Muscheler, R., Evans, M. N., Showers, W., et al. (2001). Persistent solar influence on North Atlantic climate during the Holocene. *Science*, 294(5549), 2130–2136. <https://doi.org/10.1126/science.1065680>
- Burn, M. J., & Palmer, S. E. (2014). Solar forcing of Caribbean drought events during the last millennium. *Journal of Quaternary Science*, 29(8), 827–836. <https://doi.org/10.1002/jqs.2660>
- Burn, M. J., & Palmer, S. E. (2015). Atlantic hurricane activity during the last millennium. *Scientific Reports*, 5(1), 12838. <https://doi.org/10.1038/srep12838>
- Clement, A. C., Seager, R., Cane, M. A., & Zebiak, S. E. (1996). An ocean dynamical thermostat. *Journal of Climate*, 9(9), 2190–2196. [https://doi.org/10.1175/1520-0442\(1996\)009<2190:aodt>2.0.co;2](https://doi.org/10.1175/1520-0442(1996)009<2190:aodt>2.0.co;2)
- Consortium, P. H. k. (2017). Comparing proxy and model estimates of hydroclimate variability and change over the Common Era. *Climate of the Past*, 13(12), 1851–1900. <https://doi.org/10.5194/cp-13-1851-2017>
- Coplen, T. B. (2007). Calibration of the calcite-water oxygen-isotope geothermometer at Devils Hole, Nevada, a natural laboratory. *Geochimica et Cosmochimica Acta*, 71(16), 3948–3957. <https://doi.org/10.1016/j.gca.2007.05.028>
- Deininger, M., Hansen, M., Fohlmeister, J., Schröder-Ritzrau, A., Burstyn, Y., & Scholz, D. (2021). Are oxygen isotope fractionation factors between calcite and water derived from speleothems systematically biased due to prior calcite precipitation (PCP)? *Geochimica et Cosmochimica Acta*, 305, 212–227. <https://doi.org/10.1016/j.gca.2021.03.026>
- Evans, J. L., & Webster, C. C. (2014). A variable sea surface temperature threshold for tropical convection. *Australian Meteorological and Oceanographic Journal*, 64(1), S1–S8. <https://doi.org/10.22499/2.6401.007>
- Fairchild, I. J., Borsato, A., Tooth, A. F., Frisia, S., Hawkesworth, C. J., Huang, Y., et al. (2000). Controls on trace element (Sr–Mg) compositions of carbonate cave waters: Implications for speleothem climatic records. *Chemical Geology*, 166(3), 255–269. [https://doi.org/10.1016/s0009-2541\(99\)00216-8](https://doi.org/10.1016/s0009-2541(99)00216-8)
- Fang, S. w., Khodri, M., Timmreck, C., Zanchettin, D., & Jungclaus, J. (2021). Disentangling internal and external contributions to Atlantic multidecadal variability over the past millennium. *Geophysical Research Letters*, 48(23), e2021GL095990. <https://doi.org/10.1029/2021gl095990>
- Fensterer, C., Scholz, D., Hoffmann, D., Mangini, A., & Pajón, J. M. (2010). 230Th/U-dating of a late Holocene low uranium speleothem from Cuba. *IOP Conference Series: Earth and Environmental Science*, 9, 012015. <https://doi.org/10.1088/1755-1315/9/1/012015>
- Fensterer, C., Scholz, D., Hoffmann, D., Spötl, C., Pajón, J. M., & Mangini, A. (2012). Cuban stalagmite suggests relationship between Caribbean precipitation and the Atlantic Multidecadal Oscillation during the past 1.3 ka. *The Holocene*, 0959683612449759.
- Gibert, L., Scott, G. R., Scholz, D., Budsky, A., Ferrández, C., Ribot, F., et al. (2016). Chronology for the Cueva Victoria fossil site (se Spain): Evidence for early Pleistocene Afro-Iberian dispersals. *Journal of Human Evolution*, 90, 183–197. <https://doi.org/10.1016/j.jhevol.2015.08.002>
- Govender, Y., Cuevas, E., Sternberg, L. D. S., & Jury, M. R. (2013). Temporal variation in stable isotopic composition of rainfall and groundwater in a tropical dry forest in the northeastern Caribbean. *Earth Interactions*, 17(27), 1–20. <https://doi.org/10.1175/2013ei000534.1>
- Grinsted, A., Moore, J. C., & Jevrejeva, S. (2004). Application of the cross wavelet transform and wavelet coherence to geophysical time series. *Nonlinear Processes in Geophysics*, 11(5/6), 561–566. <https://doi.org/10.5194/npg-11-561-2004>
- Haase-Schramm, A., Böhm, F., Eisenhauer, A., Dullo, W. C., Joachimski, M. M., Hansen, B., & Reitner, J. (2003). Sr/Ca ratios and oxygen isotopes from sclerosponges: Temperature history of the Caribbean mixed layer and thermocline during the Little Ice Age. *Paleoceanography*, 18(3). <https://doi.org/10.1029/2002pa000830>
- Hernández, A., Martín-Puertas, C., Moffa-Sánchez, P., Moreno-Chamarro, E., Ortega, P., Blockley, S., et al. (2020). Modes of climate variability: Synthesis and review of proxy-based reconstructions through the Holocene. *Earth-Science Reviews*, 209, 103286. <https://doi.org/10.1016/j.earscirev.2020.103286>
- Hernández Ayala, J. J. (2019). Atmospheric teleconnections and their effects on the annual and seasonal rainfall climatology of Puerto Rico. *Theoretical and Applied Climatology*, 137(3), 2915–2925. <https://doi.org/10.1007/s00704-019-02774-3>
- Hodell, D. A., Brenner, M., Curtis, J. H., & Guilderson, T. (2001). Solar forcing of drought frequency in the Maya lowlands. *Science*, 292(5520), 1367–1370. <https://doi.org/10.1126/science.1057759>
- Hosannah, N., González, J., Lunger, C., & Niyogi, D. (2019). Impacts of local convective processes on rain on the Caribbean Island of Puerto Rico. *Journal of Geophysical Research: Atmospheres*, 124(12), 6009–6026. <https://doi.org/10.1029/2018jd029825>
- Jiang, H., Muscheler, R., Björck, S., Seidenkrantz, M.-S., Olsen, J., Sha, L., et al. (2015). Solar forcing of Holocene summer sea-surface temperatures in the northern North Atlantic. *Geology*, 43(3), 203–206. <https://doi.org/10.1130/g36377.1>
- Johnson, K., Hu, C., Belshaw, N., & Henderson, G. (2006). Seasonal trace-element and stable-isotope variations in a Chinese speleothem: The potential for high-resolution paleomonsoon reconstruction. *Earth and Planetary Science Letters*, 244(1–2), 394–407. <https://doi.org/10.1016/j.epsl.2006.01.064>
- Johnson, N. C., & Xie, S.-P. (2010). Changes in the sea surface temperature threshold for tropical convection. *Nature Geoscience*, 3(12), 842–845. <https://doi.org/10.1038/ngeo1008>

- Jones, P. D., Harpham, C., Harris, I., Goodess, C. M., Burton, A., Centella-Artola, A., et al. (2016). Long-term trends in precipitation and temperature across the Caribbean. *International Journal of Climatology*, 36(9), 3314–3333. <https://doi.org/10.1002/joc.4557>
- Jungclauss, J. (2008). MPI-M Earth system modelling framework: Millennium full forcing experiment (ensemble member 1).
- Jungclauss, J. H., Lorenz, S., Timmreck, C., Reick, C., Brovkin, V., Six, K., et al. (2010). Climate and carbon-cycle variability over the last millennium. *Climate of the Past*, 6(5), 723–737. <https://doi.org/10.5194/cp-6-723-2010>
- Jury, M., Malmgren, B. A., & Winter, A. (2007). Subregional precipitation climate of the Caribbean and relationships with ENSO and NAO. *Journal of Geophysical Research*, 112(D16). <https://doi.org/10.1029/2006jd007541>
- Khalyani, A. H., Gould, W. A., Harmsen, E., Terando, A., Quinones, M., & Collazo, J. A. (2016). Climate change implications for tropical islands: Interpolating and interpreting statistically downscaled GCM projections for management and planning. *Journal of Applied Meteorology and Climatology*, 55(2), 265–282. <https://doi.org/10.1175/jamc-d-15-0182.1>
- Kilbourne, K. H., Alexander, M. A., & Nye, J. A. (2014). A low latitude paleoclimate perspective on Atlantic multidecadal variability. *Journal of Marine Systems*, 133, 4–13. <https://doi.org/10.1016/j.jmarsys.2013.09.004>
- Kilbourne, K. H., Quinn, T. M., Webb, R., Guilderson, T., Nyberg, J., & Winter, A. (2008). Paleoclimate proxy perspective on Caribbean climate since the year 1751: Evidence of cooler temperatures and multidecadal variability. *Paleoceanography*, 23(3). <https://doi.org/10.1029/2008pa001598>
- Kim, D., Lee, S. K., Lopez, H., Foltz, G. R., Misra, V., & Kumar, A. (2020). On the role of Pacific-Atlantic SST contrast and associated Caribbean Sea convection in August–October US regional rainfall variability. *Geophysical Research Letters*, 47(11), e2020GL087736. <https://doi.org/10.1029/2020gl087736>
- Klavans, J. M., Clement, A. C., Cane, M. A., & Murphy, L. N. (2022). The evolving role of external forcing in North Atlantic SST variability over the last millennium. *Journal of Climate*, 35(9), 2741–2754. <https://doi.org/10.1175/jcli-d-21-0338.1>
- Lachniet, M. S., Asmerom, Y., Polyak, V., & Bernal, J. P. (2017). Two millennia of Mesoamerican monsoon variability driven by Pacific and Atlantic synergistic forcing. *Quaternary Science Reviews*, 155, 100–113. <https://doi.org/10.1016/j.quascirev.2016.11.012>
- Landrum, L., Otto-Bliesner, B. L., Wahl, E. R., Conley, A., Lawrence, P. J., Rosenbloom, N., & Teng, H. (2013). Last millennium climate and its variability in CCSM4. *Journal of Climate*, 26(4), 1085–1111. <https://doi.org/10.1175/jcli-d-11-00326.1>
- Landsea, C. W., & Franklin, J. L. (2013). Atlantic hurricane database uncertainty and presentation of a new database format. *Monthly Weather Review*, 141(10), 3576–3592. <https://doi.org/10.1175/mwr-d-12-00254.1>
- Lapointe, F., Bradley, R. S., Francus, P., Balascio, N. L., Abbott, M. B., Stoner, J. S., et al. (2020). Annually resolved Atlantic sea surface temperature variability over the past 2,900 y. *Proceedings of the National Academy of Sciences*, 117(44), 27171–27178. <https://doi.org/10.1073/pnas.2014166117>
- Mann, M. E., Cane, M. A., Zebiak, S. E., & Clement, A. (2005). Volcanic and solar forcing of the tropical Pacific over the past 1000 years. *Journal of Climate*, 18(3), 447–456. <https://doi.org/10.1175/jcli-3276.1>
- Mann, M. E., Steinman, B. A., & Miller, S. K. (2020). Absence of internal multidecadal and interdecadal oscillations in climate model simulations. *Nature Communications*, 11(1), 49. <https://doi.org/10.1038/s41467-019-13823-w>
- Marchitto, T. M., Muscheler, R., Ortiz, J. D., Carriquiry, J. D., & van Geen, A. (2010). Dynamical response of the tropical Pacific ocean to solar forcing during the early holocene. *Science*, 330(6009), 1378–1381. <https://doi.org/10.1126/science.1194887>
- Martinez, C., Goddard, L., Kushnir, Y., & Ting, M. (2019). Seasonal climatology and dynamical mechanisms of rainfall in the Caribbean. *Climate Dynamics*, 53(1), 825–846. <https://doi.org/10.1007/s00382-019-04616-4>
- Matthes, K., Funke, B., Andersson, M. E., Barnard, L., Beer, J., Charbonneau, P., et al. (2017). Solar forcing for CMIP6 (v3. 2). *Geoscientific Model Development*, 10(6), 2247–2302. <https://doi.org/10.5194/gmd-10-2247-2017>
- Meehl, G. A., Hu, A., Castruccio, F., England, M. H., Bates, S. C., Danabasoglu, G., et al. (2021). Atlantic and Pacific tropics connected by mutually interactive decadal-timescale processes. *Nature Geoscience*, 14(1), 36–42. <https://doi.org/10.1038/s41561-020-00669-x>
- Miller, T. E. (2010). Stream pirates of the Caribbean: Panamá and Camuy Rivers in the northern Karst of Puerto Rico. *Espeleorevista Puerto Rico*, 2, 8–13.
- Moffa-Sánchez, P., Born, A., Hall, I. R., Thornalley, D. J., & Barker, S. (2014). Solar forcing of North Atlantic surface temperature and salinity over the past millennium. *Nature Geoscience*, 7(4), 275–278. <https://doi.org/10.1038/ngeo2094>
- Monroe, W. H. (1980). *Some tropical landforms of Puerto Rico*. US Government Printing Office.
- Neelin, J. D., Münnich, M., Su, H., Meyerson, J. E., & Holloway, C. E. (2006). Tropical drying trends in global warming models and observations. *Proceedings of the National Academy of Sciences*, 103(16), 6110–6115. <https://doi.org/10.1073/pnas.0601798103>
- Nyberg, J., Malmgren, B. A., Winter, A., Jury, M. R., Kilbourne, K. H., & Quinn, T. M. (2007). Low Atlantic hurricane activity in the 1970s and 1980s compared to the past 270 years. *Nature*, 447(7145), 698–701. <https://doi.org/10.1038/nature05895>
- Obert, J. C., Scholz, D., Felis, T., Brocas, W. M., Jochum, K. P., & Andreae, M. O. (2016). 230Th/U dating of Last Interglacial brain corals from Bonaire (southern Caribbean) using bulk and theca wall material. *Geochimica et Cosmochimica Acta*, 178, 20–40. <https://doi.org/10.1016/j.gca.2016.01.011>
- Obrist-Farner, J., Steinman, B. A., Stansell, N. D., & Maurer, J. (2023). Incoherency in Central American hydroclimate proxy records spanning the last millennium. *Paleoceanography and Paleoclimatology*, 38(3), e2022PA004445. <https://doi.org/10.1029/2022pa004445>
- Oster, J. L., Warken, S. F., Sekhon, N., Arienzo, M. M., & Lachniet, M. (2019). Speleothem Paleoclimatology for the Caribbean, Central America, and North America. *Quaternary*, 2(1), 5. <https://doi.org/10.3390/quat2010005>
- Otterå, O. H., Bentsen, M., Drange, H., & Suo, L. (2010). External forcing as a metronome for Atlantic multidecadal variability. *Nature Geoscience*, 3(10), 688–694. <https://doi.org/10.1038/ngeo955>
- Pausata, F. S., & Camargo, S. J. (2019). Tropical cyclone activity affected by volcanically induced ITCZ shifts. *Proceedings of the National Academy of Sciences*, 116(16), 7732–7737. <https://doi.org/10.1073/pnas.1900777116>
- Pollock, A. L., van Beynen, P. E., DeLong, K. L., Polyak, V., Asmerom, Y., & Reeder, P. P. (2016). A mid-Holocene paleoprecipitation record from Belize. *Palaeogeography, Palaeoclimatology, Palaeoecology*, 463, 103–111. <https://doi.org/10.1016/j.palaeo.2016.09.021>
- Priestley, S. C., Treble, P. C., Griffiths, A. D., Baker, A., Abram, N. J., & Meredith, K. T. (2023). Caves demonstrate decrease in rainfall recharge of southwest Australian groundwater is unprecedented for the last 800 years. *Communications Earth & Environment*, 4(1), 206. <https://doi.org/10.1038/s43247-023-00858-7>
- Rayner, N., Parker, D. E., Horton, E., Folland, C. K., Alexander, L. V., Rowell, D., et al. (2003). Global analyses of sea surface temperature, sea ice, and night marine air temperature since the late nineteenth century. *Journal of Geophysical Research*, 108(D14). <https://doi.org/10.1029/2002jd002670>
- Ridley, H. E., Asmerom, Y., Baldini, J. U. L., Breitenbach, S. F. M., Aquino, V. V., Pruffer, K. M., et al. (2015). Aerosol forcing of the position of the intertropical convergence zone since AD 1550. *Nature Geoscience*, 8(3), 195–200. <https://doi.org/10.1038/Ngeo2353>

- Rivera-Collazo, I., Winter, A., Scholz, D., Mangini, A., Miller, T., Kushnir, Y., & Black, D. (2015). Human adaptation strategies to abrupt climate change in Puerto Rico ca. 3.5 ka. *The Holocene*, 25(4), 627–640. <https://doi.org/10.1177/0959683614565951>
- Ruprich-Robert, Y., Moreno-Chamarro, E., Levine, X., Bellucci, A., Cassou, C., Castruccio, F., et al. (2021). Impacts of Atlantic multidecadal variability on the tropical Pacific: A multi-model study. *NPJ Climate and Atmospheric Science*, 4(1), 33. <https://doi.org/10.1038/s41612-021-00188-5>
- Schmidt, G. A., Jungclauss, J. H., Ammann, C. M., Bard, E., Braconnot, P., Crowley, T. J., et al. (2011). Climate forcing reconstructions for use in PMIP simulations of the last millennium (v1.0). *Geoscientific Model Development*, 4(1), 33–45. <https://doi.org/10.5194/gmd-4-33-2011>
- Scholl, M. A., & Murphy, S. F. (2014). Precipitation isotopes link regional climate patterns to water supply in a tropical mountain forest, eastern Puerto Rico. *Water Resources Research*, 50(5), 4305–4322. <https://doi.org/10.1002/2013wr014413>
- Scholl, M. A., Shanley, J. B., Zegarra, J. P., & Coplen, T. B. (2009). The stable isotope amount effect: New insights from NEXRAD echo tops, Luquillo Mountains, Puerto Rico. *Water Resources Research*, 45(12). <https://doi.org/10.1029/2008wr007515>
- Scholz, D., & Hoffmann, D. L. (2011). StalAge – An algorithm designed for construction of speleothem age models. *Quaternary Geochronology*, 6(3–4), 369–382. <https://doi.org/10.1016/j.quageo.2011.02.002>
- Schrag, D. P. (1999). Rapid analysis of high-precision Sr/Ca ratios in corals and other marine carbonates. *Paleoceanography*, 14(2), 97–102. <https://doi.org/10.1029/1998pa900025>
- Smirnov, D., Breitenbach, S., Feulner, G., Lechleitner, F., Pruffer, K., Baldini, J., et al. (2017). A regime shift in the Sun-Climate connection with the end of the Medieval Climate Anomaly. *Scientific Reports*, 7(1), 11131. <https://doi.org/10.1038/s41598-017-11340-8>
- Spötl, C. (2011). Long-term performance of the Gasbench isotope ratio mass spectrometry system for the stable isotope analysis of carbonate microsamples. *Rapid Communications in Mass Spectrometry*, 25(11), 1683–1685. <https://doi.org/10.1002/rcm.5037>
- Spötl, C., & Vennemann, T. W. (2003). Continuous-flow isotope ratio mass spectrometric analysis of carbonate minerals. *Rapid Communications in Mass Spectrometry*, 17(9), 1004–1006. <https://doi.org/10.1002/rcm.1010>
- Steidle, S. D., Warken, S. F., Schorndorf, N., Förstel, J., Schröder-Ritzrau, A., Moseley, G. E., et al. (2021). Reconstruction of Middle to Late Quaternary sea level using submerged speleothems from the northeastern Yucatán Peninsula. *Journal of Quaternary Science*, 36(7), 1190–1200. <https://doi.org/10.1002/jqs.3365>
- Steiger, N. J., Smerdon, J. E., Cook, E. R., & Cook, B. I. (2018). A reconstruction of global hydroclimate and dynamical variables over the Common Era. *Scientific Data*, 5(1), 180086. <https://doi.org/10.1038/sdata.2018.86>
- Steinman, B. A., Stansell, N. D., Mann, M. E., Cooke, C. A., Abbott, M. B., Vuille, M., et al. (2022). Interhemispheric antiphasing of neotropical precipitation during the past millennium. *Proceedings of the National Academy of Sciences*, 119(17), e2120015119. <https://doi.org/10.1073/pnas.2120015119>
- Stephenson, T. S., Vincent, L. A., Allen, T., Van Meerbeeck, C. J., McLean, N., Peterson, T. C., et al. (2014). Changes in extreme temperature and precipitation in the Caribbean region, 1961–2010. *International Journal of Climatology*, 34(9), 2957–2971. <https://doi.org/10.1002/joc.3889>
- Sullivan, R. M., van Hengstum, P. J., Coats, S. J., Donnelly, J. P., Tamalavage, A. E., Winkler, T. S., & Albury, N. A. (2021). Hydroclimate dipole drives multi-centennial variability in the western tropical North Atlantic margin during the middle and late Holocene. *Paleoceanography and Paleoclimatology*, 36(7), e2020PA004184. <https://doi.org/10.1029/2020PA004184>
- Svendsen, L., Hetzinger, S., Keenlyside, N., & Gao, Y. (2014). Marine-based multiproxy reconstruction of Atlantic multidecadal variability. *Geophysical Research Letters*, 41(4), 1295–1300. <https://doi.org/10.1002/2013gl059076>
- Swingedouw, D., Ortega, P., Mignot, J., Guilyardi, E., Masson-Delmotte, V., Butler, P. G., et al. (2015). Bidecadal North Atlantic ocean circulation variability controlled by timing of volcanic eruptions. *Nature Communications*, 6(1), 6545. <https://doi.org/10.1038/ncomms7545>
- Taylor, M. A., Enfield, D. B., & Chen, A. A. (2002). Influence of the tropical Atlantic versus the tropical Pacific on Caribbean rainfall. *Journal of Geophysical Research*, 107(C9), 3127. <https://doi.org/10.1029/2001jc001097>
- Taylor, M. A., Stephenson, T. S., Owino, A., Chen, A. A., & Campbell, J. D. (2011). Tropical gradient influences on Caribbean rainfall. *Journal of Geophysical Research*, 116(D21). <https://doi.org/10.1029/2010jd015580>
- Torrence, C., & Compo, G. P. (1998). A practical guide to wavelet analysis. *Bulletin of the American Meteorological Society*, 79(1), 61–78. [https://doi.org/10.1175/1520-0477\(1998\)079<0061:apgtwa>2.0.co;2](https://doi.org/10.1175/1520-0477(1998)079<0061:apgtwa>2.0.co;2)
- Torres-Valcárcel, A. R. (2018). Teleconnections between ENSO and rainfall and drought in Puerto Rico. *International Journal of Climatology*, 38(S1), e1190–e1204. <https://doi.org/10.1002/joc.5444>
- Treble, P. C., Baker, A., Abram, N. J., Hellstrom, J. C., Crawford, J., Gagan, M. K., et al. (2022). Ubiquitous karst hydrological control on speleothem oxygen isotope variability in a global study. *Communications Earth & Environment*, 3(1), 29. <https://doi.org/10.1038/s43247-022-00347-3>
- Tremaine, D. M., Froelich, P. N., & Wang, Y. (2011). Speleothem calcite formed in situ: Modern calibration of  $\delta^{18}\text{O}$  and  $\delta^{13}\text{C}$  paleoclimate proxies in a continuously-monitored natural cave system. *Geochimica et Cosmochimica Acta*, 75(17), 4929–4950. <https://doi.org/10.1016/j.gca.2011.06.005>
- van Beynen, P. E., Asmerom, Y., Polyak, V., Soto, L., & Polk, J. S. (2007). Variable intensity of teleconnections during the late Holocene in subtropical North America from an isotopic study of speleothem from Florida. *Geophysical Research Letters*, 34(18). <https://doi.org/10.1029/2007gl031046>
- Vásquez-Bedoya, L. F., Cohen, A. L., Oppo, D. W., & Blanchon, P. (2012). Corals record persistent multidecadal SST variability in the Atlantic Warm Pool since 1775 AD. *Paleoceanography*, 27(3). <https://doi.org/10.1029/2012pa002313>
- Vieten, R., Warken, S., Winter, A., Scholz, D., Miller, T., Spötl, C., & Schröder-Ritzrau, A. (2018). Monitoring of Cueva Larga, Puerto Rico—A first step to decode speleothem climate records. In W. B. White, J. S. Herman, E. K. Herman, & M. Rutigliano (Eds.), *Karst groundwater contamination and public health* (pp. 319–331). Springer International Publishing. [https://doi.org/10.1007/978-3-319-51070-5\\_36](https://doi.org/10.1007/978-3-319-51070-5_36)
- Vieten, R., Warken, S., Winter, A., Schröder-Ritzrau, A., Scholz, D., & Spötl, C. (2018). Hurricane impact on seepage water in Larga Cave, Puerto Rico. *Journal of Geophysical Research-Biogeosciences*, 123(3), 879–888. <https://doi.org/10.1002/2017jg004218>
- Vieten, R., Warken, S. F., Winter, A., Scholz, D., Zanchettin, D., Black, D., & Lachniet, M. (2024). A sequence of abrupt climate fluctuations in the northern Caribbean related to the 8.2 ka event. *The Holocene*, 34(3), 325–337. <https://doi.org/10.1177/09596836231211874>
- Vieten, R., Winter, A., Warken, S. F., Schröder-Ritzrau, A., Miller, T. E., & Scholz, D. (2016). Seasonal temperature variations controlling cave ventilation processes in Cueva Larga, Puerto Rico. *International Journal of Speleology*, 45(3), 259–273. <https://doi.org/10.5038/1827-806x.45.3.1983>
- Vieten, R., Zanchettin, D., Winter, A., Scholz, D., Warken, S., Black, D., et al. (2023). NOAA/WDS Paleoclimatology – Larga cave, Puerto Rico oxygen isotope and trace metal data over the past 500 years [dataset]. NOAA National Centers for Environmental Information. <https://doi.org/10.25921/1rde-t169>



- Waite, A. J., Klavans, J. M., Clement, A. C., Murphy, L. N., Liebetrau, V., Eisenhauer, A., et al. (2020). Observational and model evidence for an important role for volcanic forcing driving Atlantic multidecadal variability over the last 600 years. *Geophysical Research Letters*, *47*(23), e2020GL089428. <https://doi.org/10.1029/2020gl089428>
- Wang, C. Z., Enfield, D. B., Lee, S. K., & Landsea, C. W. (2006). Influences of the Atlantic warm pool on western hemisphere summer rainfall and Atlantic hurricanes. *Journal of Climate*, *19*(12), 3011–3028. <https://doi.org/10.1175/jcli3770.1>
- Wang, J., Yang, B., Ljungqvist, F. C., Luterbacher, J., Osborn, T. J., Briffa, K. R., & Zorita, E. (2017). Internal and external forcing of multi-decadal Atlantic climate variability over the past 1,200 years. *Nature Geoscience*, *10*(7), 512–517. <https://doi.org/10.1038/ngeo2962>
- Warken, S., Vieten, R., Winter, A., Spötl, C., Miller, T., Jochum, K. P., et al. (2020). Persistent link between Caribbean precipitation and Atlantic Ocean circulation during the Last Glacial revealed by a speleothem record from Puerto Rico. *Paleoceanography and Paleoclimatology*, *30*(11). <https://doi.org/10.1029/2020PA003944>
- Warken, S. F., Kuchalski, L., Schröder-Ritzrau, A., Vieten, R., Schmidt, M., Hoepker, S., et al. (2022). The impact of seasonal and event-based infiltration on transition metals (Cu, Ni, Co) in tropical cave drip waters. *Rapid Communications in Mass Spectrometry*, e9278. <https://doi.org/10.1002/rcm.9278>
- Warken, S. F., Schorndorf, N., Stinnesbeck, W., Hennhoefler, D., Stinnesbeck, S. R., Förstel, J., et al. (2021). Solar forcing of early Holocene droughts on the Yucatán peninsula. *Scientific Reports*, *11*(1), 13885. <https://doi.org/10.1038/s41598-021-93417-z>
- Warken, S. F., Weissbach, T., Kluge, T., Vonhof, H., Scholz, D., Vieten, R., et al. (2022). Last glacial millennial-scale hydro-climate and temperature changes in Puerto Rico constrained by speleothem fluid inclusion  $\delta$  18 O and  $\delta$  2 H values. *Climate of the Past*, *18*(1), 167–181. <https://doi.org/10.5194/cp-18-167-2022>
- Winter, A., Miller, T., Kushnir, Y., Sinha, A., Timmermann, A., Jury, M. R., et al. (2011). Evidence for 800 years of North Atlantic multi-decadal variability from a Puerto Rican speleothem. *Earth and Planetary Science Letters*, *308*(1–2), 23–28. <https://doi.org/10.1016/j.epsl.2011.05.028>
- Winter, A., Zanchettin, D., Lachniet, M., Vieten, R., Pausata, F. S. R., Ljungqvist, F. C., et al. (2020). Initiation of a stable convective hydro-climatic regime in Central America circa 9000 years BP. *Nature Communications*, *11*(1), 716. <https://doi.org/10.1038/s41467-020-14490-y>
- Winter, A., Zanchettin, D., Miller, T., Kushnir, Y., Black, D., Lohmann, G., et al. (2015). Persistent drying in the tropics linked to natural forcing. *Nature Communications*, *6*(1), 7627. <https://doi.org/10.1038/ncomms8627>
- Wright, K. T., Johnson, K. R., Bhattacharya, T., Marks, G. S., McGee, D., Elsbury, D., et al. (2022). Precipitation in Northeast Mexico primarily controlled by the relative warming of Atlantic SSTs. *Geophysical Research Letters*, *49*(11), e2022GL098186. <https://doi.org/10.1029/2022gl098186>
- Yang, Q., Scholz, D., Jochum, K. P., Hoffmann, D. L., Stoll, B., Weis, U., et al. (2015). Lead isotope variability in speleothems—A promising new proxy for hydrological change? First results from a stalagmite from western Germany. *Chemical Geology*, *396*, 143–151. <https://doi.org/10.1016/j.chemgeo.2014.12.028>
- Yang, W., Wallace, E., Vecchi, G. A., Donnelly, J. P., Emile-Geay, J., Hakim, G. J., et al. (2024). Last millennium hurricane activity linked to endogenous climate variability. *Nature Communications*, *15*(1), 816. <https://doi.org/10.1038/s41467-024-45112-6>
- Zanchettin, D., Bothe, O., Graf, H. F., Lorenz, S. J., Luterbacher, J., Timmreck, C., & Jungclaus, J. H. (2013). Background conditions influence the decadal climate response to strong volcanic eruptions. *Journal of Geophysical Research: Atmospheres*, *118*(10), 4090–4106. <https://doi.org/10.1002/jgrd.50229>
- Zanchettin, D., Bothe, O., Graf, H. F., Omrani, N. E., Rubino, A., & Jungclaus, J. H. (2016). A decadal delayed response of the tropical Pacific to Atlantic multidecadal variability. *Geophysical Research Letters*, *43*(2), 784–792. <https://doi.org/10.1002/2015gl067284>
- Zanchettin, D., Bothe, O., Müller, W., Bader, J., & Jungclaus, J. H. (2014). Different flavors of the Atlantic multidecadal variability. *Climate Dynamics*, *42*(1–2), 381–399. <https://doi.org/10.1007/s00382-013-1669-0>
- Zanchettin, D., Bothe, O., Rubino, A., & Jungclaus, J. H. (2016). Multi-model ensemble analysis of Pacific and Atlantic SST variability in unperturbed climate simulations. *Climate Dynamics*, *47*(3–4), 1073–1090. <https://doi.org/10.1007/s00382-015-2889-2>
- Zanchettin, D., Fang, S.-W., Khodri, M., Omrani, N.-E., Rubineti, S., Rubino, A., et al. (2023). Thermohaline patterns of intrinsic Atlantic multidecadal variability in MPI-ESM-LR. *Climate Dynamics*, *61*(5–6), 1–23. <https://doi.org/10.1007/s00382-023-06679-w>
- Zhang, R., & Delworth, T. L. (2007). Impact of the Atlantic multidecadal oscillation on north Pacific climate variability. *Geophysical Research Letters*, *34*(23), L23708. <https://doi.org/10.1029/2007gl031601>
- Zhang, R., Delworth, T. L., Sutton, R., Hodson, D. L., Dixon, K. W., Held, I. M., et al. (2013). Have aerosols caused the observed Atlantic multidecadal variability? *Journal of the Atmospheric Sciences*, *70*(4), 1135–1144. <https://doi.org/10.1175/jas-d-12-0331.1>

## References From the Supporting Information

- Cheng, H., Edwards, R. L., Hoff, J., Gallup, C. D., Richards, D. A., & Asmerom, Y. (2000). The half-lives of uranium-234 and thorium-230. *Chemical Geology*, *169*(1–2), 17–33. [https://doi.org/10.1016/s0009-2541\(99\)00157-6](https://doi.org/10.1016/s0009-2541(99)00157-6)